Hindawi Publishing Corporation
Advances in Mechanical Engineering
Volume 2013, Article ID 765627, 7 pages
http://dx.doi.org/10.1155/2013/765627

Research Article

Fast Numerical Solutions of Gas-Particle Two-Phase Vacuum Plumes

ZhaoXin Ren, Bing Wang, and Huiqiang Zhang

School of Aerospace, Tsinghua University, Beijing 100084, China

Correspondence should be addressed to Bing Wang; wbing@tsinghua.edu.cn

Received 23 July 2013; Accepted 16 September 2013

Academic Editor: Qiang Wang

The free molecule point source and Simons models coupled to the particle Lagrangian trajectory model are employed, respectively, to establish the fast solving method for gas-particle two-phase vacuum plumes. Density, velocity and temperature distributions of gas phase, and velocity and temperature of particles are solved to present the flow properties of two-phase plumes. The method based on free molecule point source model predicts the velocity and temperature distributions of vacuum plumes more reasonably and accurately than the Simons model. Comparisons of different drag coefficients show that Loth's drag formula can calculate exactly particle initial acceleration process for high Re_r and M_r two-phase flows. The response characteristics of particles along their motion paths are further analyzed. Smaller particles can easily reach momentum equilibrium, while larger ones accelerate very difficultly. The thermal response is more relaxed than momentum response for different particle sizes. The present study is guidable to consider the effects of two-phase plumes on spacecraft in engineering.

1. Introduction

Spacecraft engines generate vacuum plumes, which result in dramatic impacts on components of spacecraft and hence a series of serious damage. Therefore, it is necessary to accurately evaluate the impact force, moment, and heat fluxes induced by plumes and supply theoretical basis and guidelines for flight control as well as protective designs of sensitive optical surface for spacecrafts. Especially, a two-phase vacuum plume can exist, if combustion exhaust includes particles or droplets. The effects of two-phase plumes on spacecrafts are different due to the presence of particle phase.

The investigation approaches on plumes are mainly by means of ground experiments, numerical simulation, and theoretical analysis. For nozzle exhaust flows of rocket engines, there are plants of ground experimental data, which can be referred by the researchers for establishing experience formulas. But it is very difficult and expensive to maintain the vacuum environments in experiments. Direct Simulation of Mento Carlo (DSMC) method is an effective means to simulate nozzle plumes. However, because the development of vacuum plume experiences the continuum, slip, transition, and free molecular flows successively, the calculation cost is also very high for DSMC. It is necessary to establish models for realizing the fast calculation and analysis of plumes, which are valuable to meet the requirements in engineering.

For engineering calculation methods, Simons proposed a simple approach, regarding the nozzle flow of rocket engine as a point source, which is also called as the cosine method [1]. Amount of experimental data is used to modify and improve this theoretical model. The other methods proposed by researchers based on the free molecule flow are more complex than Simons method [2]. There are several typical works using the free molecule flow model. Noller applied the solid angle method to calculate the density field of the nozzle plume [3]. Brook predicted the annular density fields induced by the sealing leakage of cabin door [4]. Woronowicz and Ghaarian calculated the density and velocity distributions through expanding the single point source to a series of uniform point sources [5]. Cheng et al. [6] then improved Woronowize's method, considering the flow nonuniform of nozzle exit. Cai and Boyd [7, 8] proposed approaches to solve two-dimensional collisionless round plumes. In addition, Cai and Wang regarded that the method of Cai and Boyd is more reasonable than the Simons method after carefully comparing the calculations of a vacuum plume [9]. However, establishing

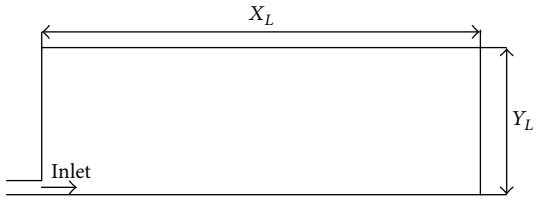

Figure 1: Schematic diagram of calculation model and computation domain.

a method based on the free molecule flow and applying it on calculations of gas-particle two-phase vacuum plumes are not yet done.

The motion of a particle in the rarefied flow is different from in the continuum flow. The drag is the main force for particle motion, but the calculation of drag coefficient needs a modification in compressible and rarefied flows. Loth indicated that the rarefaction dominates the modifications of drag force for low slip or small particle Reynolds number flows, but the compressibility dominates the effects on drag force for high particle Reynolds number flows [10]. However, there are few investigations on two-phase vacuum plumes utilizing particle Lagrangian tracking method.

Therefore, this paper performs numerical computations of vacuum plumes employing the free molecule point source method and Simons method, respectively. Based on the single phase plume, particles are released and tracked by means of Lagrangian trajectory model. The particle acceleration and thermal response process are analyzed in two-phase vacuum plumes. The comparisons of different drag coefficient models are also carried out in the present study.

2. Physical Model and Numerical Method

2.1. Computation Method of Gas-Phase Plume

2.1.1. Free Molecule Point Source Model. For a given point source of nozzle n, the density fields are calculated by, in the free molecule point source model proposed by Woronowicz,

$$\rho_g^n(\mathbf{x}) = \frac{\beta_n \dot{m}_n \cos\phi_n}{A_n \pi r_n^2} \times e^{w_n^2 - s_n^2} \cdot \left(w_n e^{-w_n^2} + \left(\frac{1}{2} + w_n^2\right) \times \sqrt{\pi}\left(1 + \operatorname{erf}\left(w_n^2\right)\right)\right), \tag{1}$$

where $\mathbf{x}$ is the position vector from a space point to the nozzle exit center point, $\beta_n = 1/\sqrt{2RT_{en}}$ and speed ratio $s_n = \beta_n u_{en}$. $\dot{m}_n(t)$ is mass flux of nozzle flow. ϕ_n is the inclined angle between the position vector $\mathbf{r}_n$ and the normal direction of nozzle exit plane $\widehat{n}$. A_n is a normalization factor, whose calculation formula can be referred in [5]. $w_n = s_n \cos\theta_n$, where angle θ_n is measured between the exit velocity at nth nozzle and $\mathbf{r}_n$.

Therefore, the velocity u_g at $\mathbf{x}$ and the translational temperature $T_{g,t}$ are calculated by, respectively [6],

$$u_g^n(\mathbf{x}) = \frac{B_n\left(\left(1 + w_n^2\right)e^{-w_n^2} + \left(3/2 + w_n^2\right) w_n C_n\right) \cdot \left(\mathbf{r}_n / r_n\right)}{\rho_g^n(\mathbf{x})},$$

$$T_{g,t}^n(\mathbf{x}) = \frac{1}{3R}\left(\frac{1}{\beta_n} B_n \left(\left(\frac{5}{2} w_n + w_n^3\right) e^{-w_n^2} + \left(\frac{3}{4} + 3w_n^2 + w_n^4\right) C_n\right) \times \left(\rho_g^n(\mathbf{x})\right)^{-1} - \left(u_g^n(\mathbf{x})\right)^2\right), \tag{2}$$

where $B_n = \dot{m}_n \cos\phi_n / A_n \pi r_n^2 \cdot e^{w_n^2 - s_n^2}$ and $C_n = \sqrt{\pi}(1 + \operatorname{erf}(w_n))$. γ is the ratio of specific heat capacity.

Finally, the superposition of results for all point sources is taken as the ultimate forecasting value of the velocity and temperature, respectively,

$$u_g(\mathbf{x}) = \frac{\sum_{n=1}^{N} \rho_g^n(\mathbf{x})\, u_g^n(\mathbf{x})}{\rho_g(\mathbf{x})},$$
$$T_{g,t}(\mathbf{x}) = \frac{\sum_{n=1}^{N} \rho_g^n(\mathbf{x})\, T_{g,t}^n(\mathbf{x})}{\rho_g(\mathbf{x})}. \tag{3}$$

2.1.2. Simons Model. Simons regarded that the plume is developed from a virtual point source if the exhaust flow domain is very larger than the nozzle scale. The calculation of density reads as

$$\frac{\rho_g(r,\theta)}{\rho^*} = A\left(\frac{R^*}{r}\right)^2 f(\theta), \tag{4}$$

where r and θ define the space position and ρ^* is the density of the throat with a radius of R^*. A is the plume constant, depending on the nozzle configuration and gas prosperities. The $f(\theta)$ is expressed as, in the isentropic core region,

$$f(\theta) = \left(\cos\left(\frac{\pi}{2} \cdot \frac{\theta}{\theta_\infty}\right)\right)^{2/(\gamma-1)} \quad 0 \le \theta \le \theta_0, \tag{5}$$

while $f(\theta)$ is expressed as, in the expansion regions of boundary layer,

$$f(\theta) = f(\theta_0)\exp\left(-\beta(\theta - \theta_0)\right) \quad \theta_0 \le \theta \le \theta_\infty, \tag{6}$$

where β is the coefficient constant, θ_0 is the limit deflection angle of the flow in the isentropic core region, and θ_∞ is the limit deflection angle of the nozzle flow. They can be approximately obtained according to the Prandtl-Meyer function. All the other physical variables can be calculated by the isentropic equations.

2.2. Calculation Method of Particle Phase.

Because the drag force is in several orders of magnitude larger than the

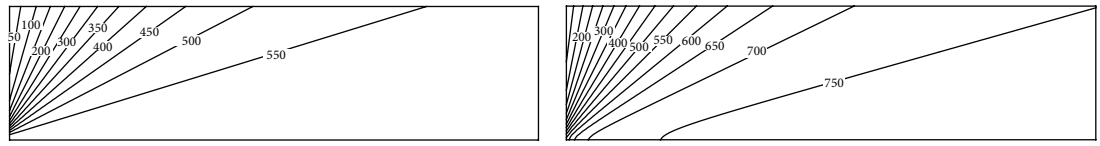

(a) (b)

Figure 2: Streamwise velocity (m/s) ((a) results obtained by free molecular point source method, (b) results obtained by Simons method).

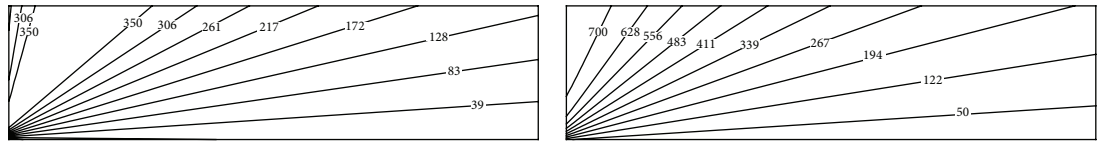

(a) (b)

Figure 3: Transverse velocity (m/s) ((a) results obtained by free molecular point source method, (b) results obtained by Simons method).

other forces imposing on a particle, the particle Lagrangian trajectory model reads as

$$\frac{d\mathbf{x}_p}{dt} = u_p,$$
$$\frac{du_p}{dt} = \frac{C_D \mathrm{Re}_r}{24\tau_u}\left(u_g - u_p\right), \tag{7}$$

where $\mathbf{x}_p$ is the particle position vector; u_p is the particle velocity; u_g is the gas-phase velocity at the particle position. $\mathrm{Re}_r = \rho_g d_p |u_p - u_g|/\mu_g$ is the particle Reynolds number, and $\tau_u = \rho_g d_p^2/(18\mu_g)$ is the aerodynamics relaxation time. ρ_g is gas density, μ_g is gas viscosity, and d_p is particle diameter.

C_D is the drag coefficient, with different corrections as follows:

(1) Millikan's expression [11]:

$$C_{D,\mathrm{Kn},\mathrm{Re}_r} = C_{D,\mathrm{stokes}} f(\mathrm{Kn}) = \frac{24}{\mathrm{Re}_r}\frac{1}{1 + \mathrm{Kn}\left(2.492 + 0.84\exp\left(-1.74/\mathrm{Kn}\right)\right)}, \tag{8}$$

(2) Clift's expression [12]:

$$f(\mathrm{Kn}) = \frac{1}{1 + \mathrm{Kn}\left(2.514 + 0.8\exp\left(-0.55/\mathrm{Kn}\right)\right)}, \tag{9}$$

with a correction by Schiller-Naumann:

$$C_{D,\mathrm{Kn},\mathrm{Re}_r} = \frac{24}{\mathrm{Re}_r}\left(1 + 0.15\mathrm{Re}_r^{0.687}\right) \times \frac{1}{1 + \mathrm{Kn}\left(2.514 + 0.8\exp\left(-0.55/\mathrm{Kn}\right)\right)}, \tag{10}$$

(3) Loth's expression [10]:

$$C_D = \frac{C_{D,\mathrm{Kn},\mathrm{Re}_r}}{1 + M_r^4} + \frac{M_r^4 C_{D,FM}}{1 + M_r^4}, \tag{11}$$

where $C_{D,\mathrm{Kn},\mathrm{Re}_r}$ is the same as (10) and $C_{D,FM}$ is formulated as

$$C_{D,FM} = \left(1 + 2S^2\right)\frac{\exp\left(-S^2\right)}{S^3\sqrt{\pi}} + \frac{4S^4 + 4S^2 - 1}{2S^4}\mathrm{erf}(S) + \frac{2}{3S}\sqrt{\pi\frac{T_p}{T_g}}. \tag{12}$$

In the above expressions, $M_r^4 = |u_p - u_g|/a_g$ is the relative Mach number, $\mathrm{Kn} = \sqrt{\pi\gamma/2}(M_r^4/\mathrm{Re}_r)$ is the Knudsen number, and $S = \sqrt{\gamma/2}M_r^4$ is the molecule velocity ratio.

The overall tendency of particle drag coefficient decreases with an increase of particle Reynolds number Re_r as shown in [10]. Before the Nexus point, $\mathrm{Re}_r = 45$, the rarefaction effects are leading, whereas after that the compressibility effects dominate. If rarefaction effects are stronger, drag decreases with an increase of Kn number. However, if compressibility effects are stronger, drag increases with an increase of M_r number.

The rarefaction effects on heat transfer between gas and particles are also considered. The particle temperature equation reads as

$$\frac{dT_p}{dt} = \frac{\mathrm{Nu}}{2}\frac{\left(T_g - T_p\right)}{\tau_T}, \tag{13}$$

where $\tau_T = \rho_p c_p d_p^2/(12k_f)$ is the thermal relaxation time, ρ_p is particle density, c_p is the specific heat capacity, and k_f is the heat conduction coefficient.

The Nusselt number with a correction is expressed as [13]

$$\mathrm{Nu} = \frac{\mathrm{Nu}_0}{1 + 3.42\mathrm{Nu}_0\left(M_r/\mathrm{Re}_p\mathrm{Pr}\right)}, \tag{14}$$

where $\mathrm{Nu}_0 = 2 + 0.6\mathrm{Re}_r^{0.5}\mathrm{Pr}^{0.33}$ and $\mathrm{Pr} = \nu/\alpha$.

The u_g and T_g in (7) and (13) are obtained by a fourth-order interpolation method.

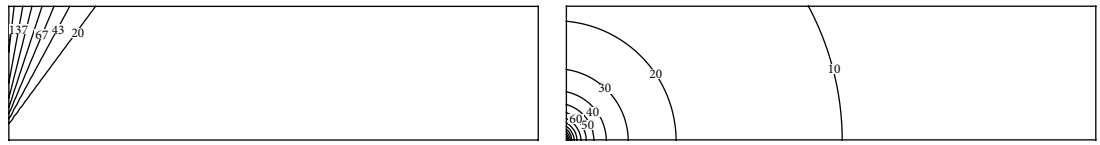

(a) (b)

Figure 4: Temperature (K) ((a) results obtained by free molecular point source method, (b) results obtained by Simons method).

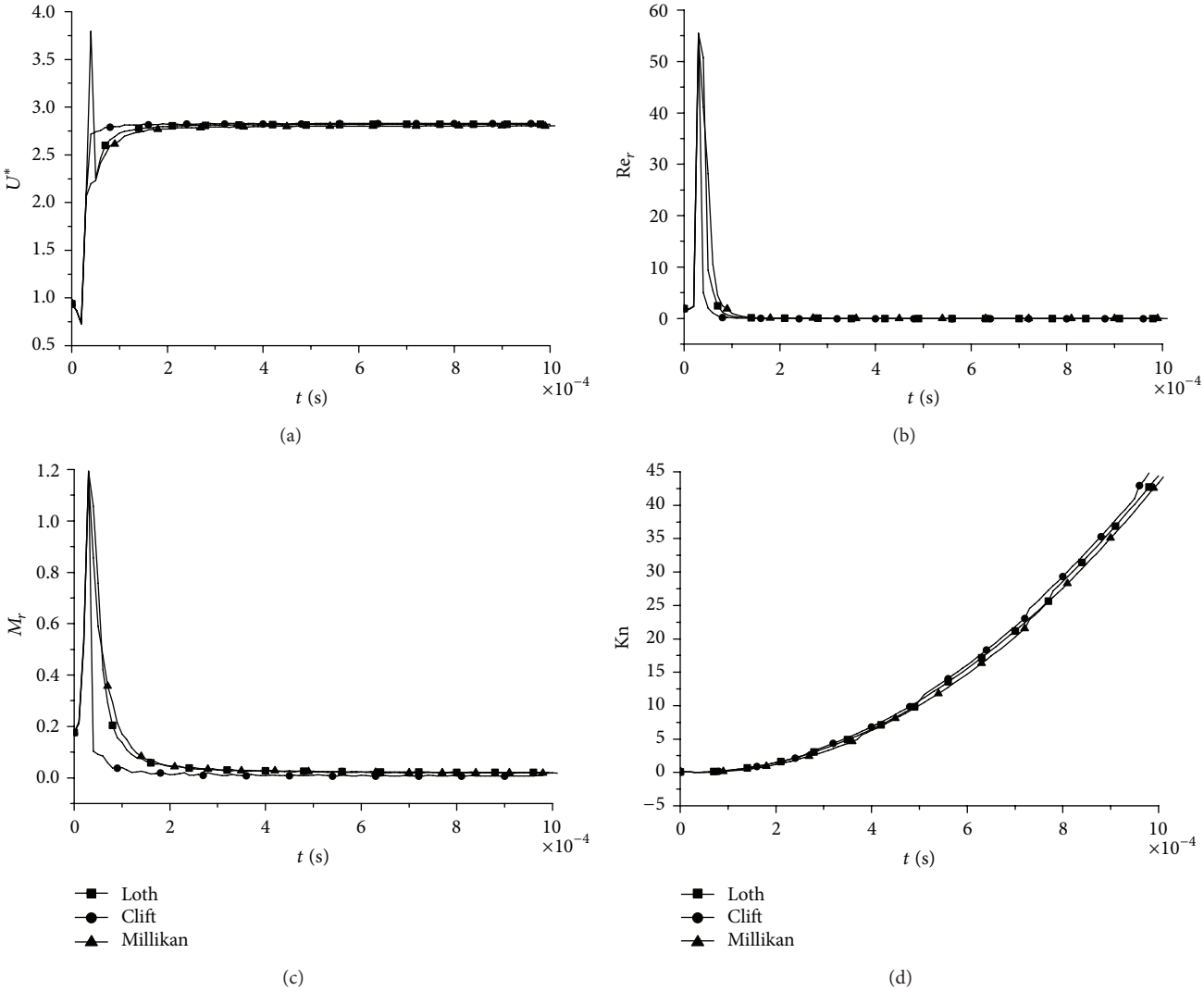

Figure 5: The variations of physical variables of U^*, Re_r, M_r, and Kn along a particle trajectory by means of free molecule point source method.

3. Results and Discussions

The physical model and computation domain are shown in Figure 1. Half of the nozzle with axisymmetric configuration is taken in the present study. The outlet physical variables of nozzle flow are obtained by solving Navier-Stokes governing equations. The initial calculation parameters are shown in Table 1.

Table 1: The parameters in the calculations.

Computational domain (m × m)	0.4 × 0.1
Radius of nozzle exit R_e (m)	0.0045
Nozzle exit velocity u_e (m/s)	209.28

3.1. Gas-Phase Plumes. The streamwise, transverse velocity, and temperature distributions of gas-phase plumes are shown in Figures 2, 3, and 4, respectively. We first analyze the results obtained by the free molecule point source method. The streamwise velocity is larger close to the nozzle axis, but its gradients decrease. The transverse velocity is distributed

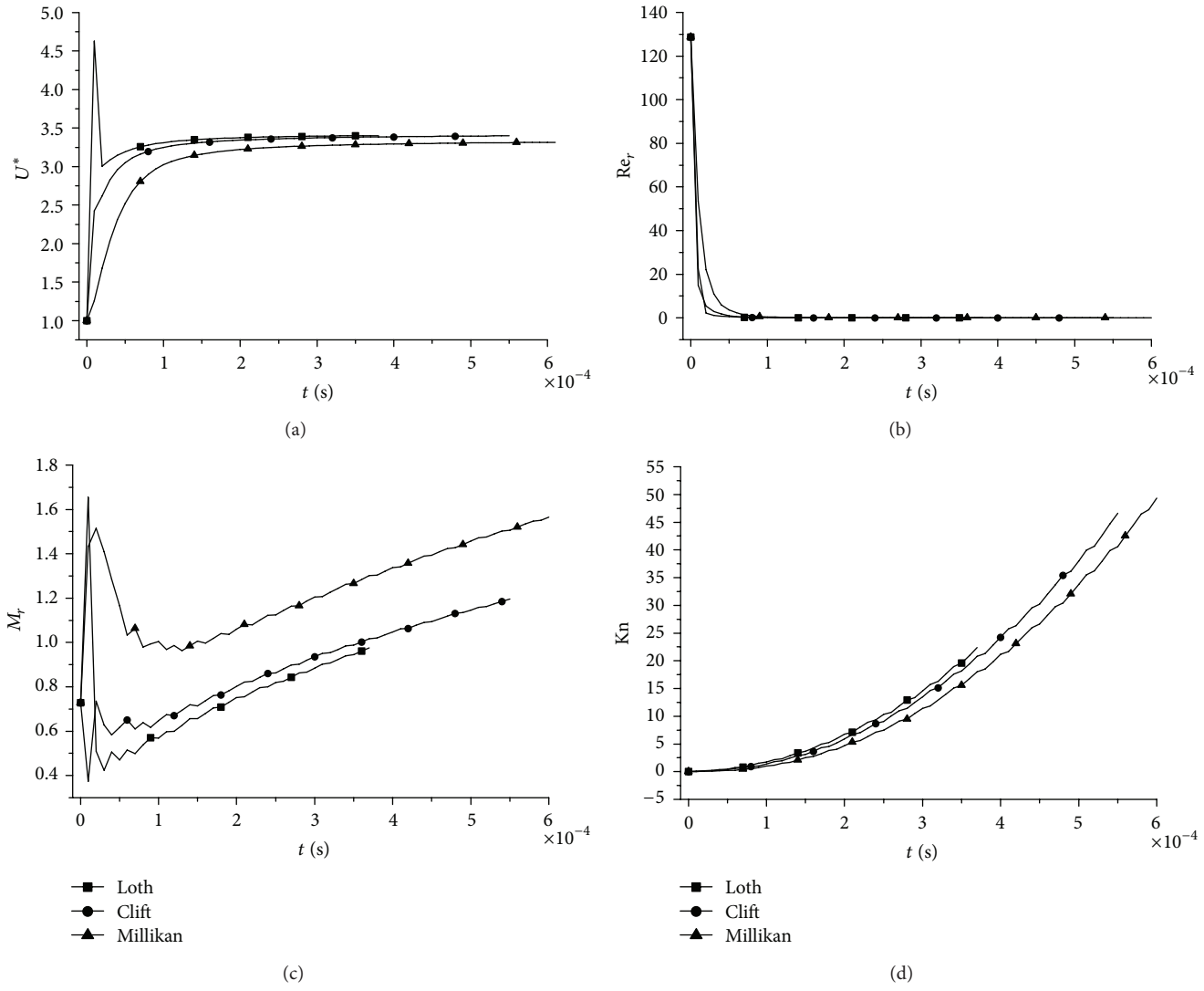

Figure 6: The variations of physical variables of U^*, Re_r, M_r, and Kn along a particle trajectory by means of Simons method.

within a specific deflection angle with its maximum value. The temperature remains unchanged within a fan-shaped region. Away from the axis, the temperature increases, and the gradients become larger. The exhaust expands outside the nozzle, and both the streamwise and transverse velocities increase, but the temperature decreases.

The results of velocities obtained by Simons method are similar to those predicted by free molecule point source method. But the former values are larger. Closer to the axis of nozzle, the streamwise velocity is larger, but its gradients are smaller; however, the transverse velocity is smaller.

On the contrary, the predictions of temperature are quite different for two methods. The common point is that, along the radial direction, the temperature of gas and its gradients both decrease due to the free expansion of exhaust in vacuum.

3.2. Particle Phase Motion. The steady drag model is not applicable for rarefied flows since the drag coefficients decrease because of rarefaction effects. In the present study, a single particle is tracked in the plume by employing the model of (8)–(11), respectively. The particle parameters are shown in Table 2.

Table 2: Particle parameters.

Density ρ_p (kg/m^3)	2700
Diameter d_p (m^{-6})	2, 20, 200
Initial velocity $u_{p,e}$ (m/s)	209.28
Initial temperature $T_{p,e}$ (K)	105.36

Figure 5 shows the variations of physical variables of U^*, Re_r, M_r, and Kn along a particle trajectory by means of free molecule point source method. If a particle has the same initial velocity and the same inlet position, its velocity is different in the beginning, but same in the end using different drag coefficient models. The velocity calculated by Loth's model has the most significant acceleration in the beginning. Re_r or M_r has the similar tendency. But the velocity difference between two phases cannot be obtained by means of Milikan's

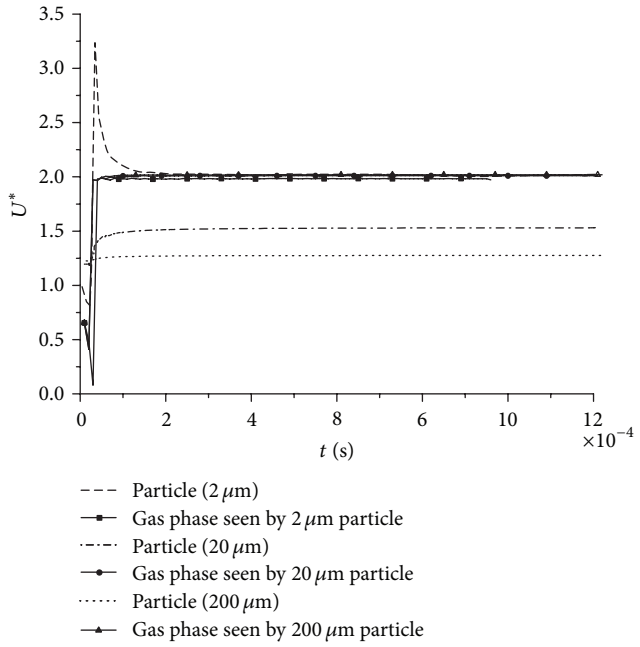

Figure 7: Momentum response of particle with different diameter to gas phase.

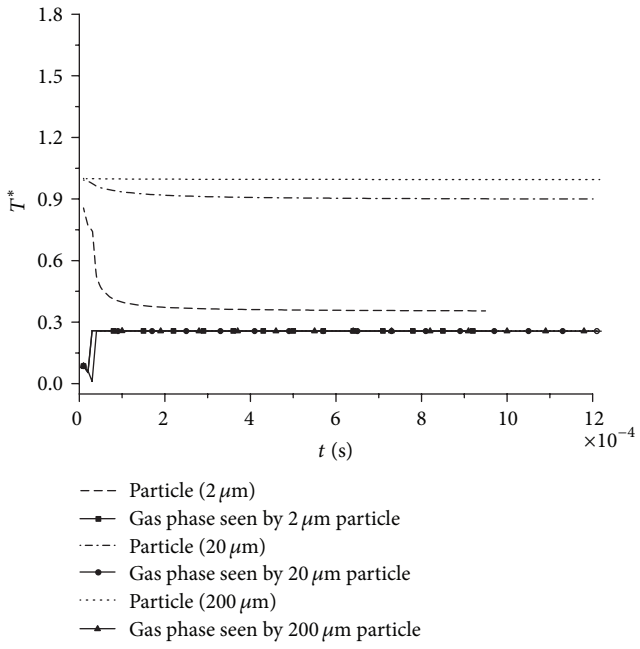

Figure 8: Thermal response of particle with different diameter to gas phase.

or Clift's models. In the initial acceleration process, the maximum value of Re_r is larger than 45 (Nexus point), so the particle motion is influenced by flow compressibility. This then show that the model of Milikan or Clift cannot yield the calculation of particle motion if the flow has very strong compressibility. The variation of Kn number shows that the rarefaction effects become stronger away from the nozzle exit. Hence, the drag coefficient model must be applied in a wide range of Kn number because the particle experiences the continuum, slip, transition, and free molecule flow successively. Compared with the models of Milikan and Clift, Loth's model has the best applicability for two-phase plumes.

From results of Simons method, as displayed in Figure 6, only Loth's model can reflect the response of particles to high Re_r gas flows. Different drag coefficient models result in particles' different variable motions, but they finally keep different constant velocities. The difference of ultimate velocity is due to the disparity of particle motion trajectories and different surrounding gas velocity. Since the gas-phase temperature surrounding a particle decreases gradually when the particle moves downstream, the variations of M_r are complex, but, in general, they increase finally.

The momentum and thermal responses of different sized particles to gas phase are shown in Figures 7 and 8, respectively. With an increase of particle diameter, both the velocity and temperature differences between two phases increase. It is shown that the momentum and thermal responses to gas phase become difficult for large particles. The 200 μm particle almost keeps its initial velocity and temperature as it moves downstream. The 2 μm particle has the fastest response and obtains a consistent velocity with the gas-phase quickly. However, even if the 2 μm particle reaches the momentum equilibrium, it is still very difficult to realize thermal equilibrium with the gas phase. It means that the thermal response is more relaxed than the momentum response.

4. Conclusions

This paper successfully performed a fast numerical calculation of two-phase vacuum plumes. The free molecule point source and Simons models coupled with particle Lagrangian trajectory model were employed, respectively. Different drag coefficient models were considered in the calculation to reveal their effects on particles' motion in rarified flows. The following conclusions were obtained.

Both the free molecule point source and Simons models could compute similar velocity distribution in plumes, but the former predicted better. The vacuum plume experienced continuum, slip, transition, and free molecule flow. The drag coefficient model needed applicative modifications, considering both rarefaction and compressibility effects. The model proposed by Loth showed a better applicability, with better predictions for higher Re_r and M_r flows.

Particles were immediately accelerated by the dense plumes close to the nozzle exit. The momentum and thermal responses became more relaxed as particles' diameter increased. The thermal equilibrium was more difficult to achieve than the momentum equilibrium.

References

[1] G. A. Simons, "Effects of nozzle boundary layers on rocket exhaust plumes," *AIAA Journal*, vol. 10, no. 11, pp. 1534–1535, 1972.

[2] R. Narasimha, "Collisionless expansion of gases into vacuum," *Journal of Fluid Mechanics*, vol. 12, no. 2, pp. 294–308, 1962.

[3] H. G. Noller, "Approximate calculation of expansion of gas from nozzles into high vacuum," *Journal of Vacuum Science and Technology*, vol. 3, no. 4, p. 202, 1966.

[4] J. W. Brook, "Density field of directed free-molecular flow from an annulus," *Journal of Spacecraft and Rockets*, vol. 6, no. 6, pp. 755–757, 1969.

[5] M. Woronowicz and S. Ghaarian, "Highlights of transient plume impingement model validation and applications," in *Proceedings of the 42nd AIAA Thermophysics Conference (AIAA '11-3772)*, June 2011.

[6] X. L. Cheng, Q. Wang, and X. Q. Yan, "Application of the free molecule point source model to the plume field with nonuniform outlet conditions," *Acta Aerodynamica Sinica*, vol. 22, no. 1, pp. 97–100, 2004 (Chinese).

[7] C. Cai, *Theoretical and numerical studies of plume flows inside vacuum chambers [Ph.D. thesis]*, Department of Aerospace Engineering, University of Michigan, Ann Arbor, Mich, USA, 2005.

[8] C. Cai and I. D. Boyd, "Theoretical and numerical study of free-molecular flow problems," *Journal of Spacecraft and Rockets*, vol. 44, no. 3, pp. 619–624, 2007.

[9] C. Cai and I. D. Boyd, "Collisionless gas expanding into vacuum," *Journal of Spacecraft and Rockets*, vol. 44, no. 6, pp. 1326–1330, 2007.

[10] E. Loth, "Compressibility and rarefaction effects on drag of a spherical particle," *AIAA Journal*, vol. 46, no. 9, pp. 2219–2228, 2008.

[11] R. A. Millikan, "Coefficients of slip in gases and the law of reflection of molecules from the surfaces of solids and liquids," *Physical Review*, vol. 21, no. 3, pp. 217–238, 1923.

[12] R. Clift, J. R. Grace, and M. E. Weber, *Bubbles, Drops and Particles*, Academic Press, New York, NY, USA, 1978.

[13] L. Kavanau, "Heat transfer from spheres to a rarefied gas in subsonic flow," *Journal of Heat Transfer-Transactions of the ASME*, vol. 77, pp. 617–623, 1955.